Total integral and ejected-energy differential cross sections for the electron-impact ionization of lithium

J. Colgan and M. S. Pindzola
Department of Physics, Auburn University, Auburn, Alabama 36849

D. M. Mitnik and D. C. Griffin
Department of Physics, Rollins College, Winter Park, Florida 32789
(Received 19 December 2000; published 8 May 2001)

Time-dependent close-coupling calculations of the electron-impact ionization of lithium are presented and compared to experiment and other recent theoretical calculations. Total integral cross sections are found to be in excellent agreement with the previous converged close-coupling calculations of Bray [J. Phys. B **28**, L247 (1995)], but are substantially lower than the only low-energy region experimental results of Zapesochnyi and Aleksakhin [Sov. Phys. JETP **28**, 41 (1969)]. Ejected-energy differential cross sections are presented for incident energies of 10 eV, 15 eV, 20 eV, and 25.4 eV. At 25.4 eV, the time-dependent close-coupling results are found to be in only moderately good agreement with the converged close-coupling results of Bray *et al.* [J. Phys. B **32**, 4309 (1999)]. A study is also made of the convergence of the spin asymmetry parameter as a function of orbital angular momentum. The final time-dependent result for the spin asymmetry parameter at an incident energy of 15 eV is found to be in excellent agreement with the converged close-coupling results of Bray [J. Phys. B **28**, L247 (1995)], but is slightly lower than the experiment of Baum *et al.* (1985).

I. INTRODUCTION

Electron-impact ionization is one of the basic collision processes for atoms and molecules and is studied not only for its intrinsic importance, but also for a wide range of applications, such as in fusion plasma diagnostics, radiation effects on materials, and astrophysics. Lithium is one of the more important diagnostic elements for controlled fusion, and recently there has been much interest in its use as a liquid metal wall in tokamaks [1]. This may overcome the first-wall problems in fusion devices and can also cause the flux of particles recycling back from the wall and refueling the plasma to become very low. It is important, therefore, to have accurate data for electron-impact ionization processes.

In recent years, there has been good progress in theoretical calculations for electron-impact ionization of the lithium-like atomic ions. Systematic studies have been made using convergent close-coupling, R matrix with pseudostates, and time-dependent close-coupling theory [2–7]. These theoretical calculations vary in their agreement with experimental measurements. The nonperturbative calculations [2–4] for the electron-impact ionization of Be^+ are in agreement with each other but are both substantially lower than experiment [8]. However, nonperturbative calculations for the electron-impact ionization of B^{2+} [2,5,6] are in good agreement with each other and with experiment [7]. Calculations on lithium, extending this sequence, should help in the understanding of these anomalies.

For electron-impact ionization of lithium, reasonable agreement exists between the distorted-wave calculations of Younger [9] and older experimental measurements [10–12]. Convergent close-coupling calculations [2] are substantially lower than the experimental measurements (which were all done at least 25 years previously) at all energies by up to 20%. There has been little information available to date about these differential cross sections for electron scattering by lithium; only the calculation by Bray *et al.* [13] has yielded ejected-energy differential cross sections at two incident electron energies. No experimental measurements appear to be available at this time. In contrast, there has been recent experimental measurements of triple energy and angle differential cross sections for electron ionization of lithium [14,15] that have shown good agreement with theoretical calculations [13,16,17].

This paper therefore aims to fill these gaps by calculating total integral and ejected-energy differential cross sections for the electron-impact ionization of lithium. We will check our total integral cross sections against previous converged close-coupling results, which are substantially lower than experiment. There have also been concerns over the calculation of ejected-energy differential cross sections using the convergent close-coupling method. In recent calculations of the triply differential cross section for electron-impact ionization of hydrogen, the exterior complex-scaling method [18] and the convergent close-coupling method [19] agree very well in shape, but not in magnitude. These differences have been traced to differences in the calculation of the ejected-energy differential cross section at equal energy sharing. A recent study has made an effort to resolve this difference by calculation of only the $L=0, S=0$ component of the full electron-hydrogen problem [20]. Therefore, an independent calculation of the ejected-energy differential cross section for lithium should prove useful.

In this paper, we use a time-dependent close-coupling method [21,22] that has met with considerable success in recent years in the calculation of the electron-impact ionization of atomic systems. Good agreement has been found between experiment and time-dependent close-coupling theoretical calculations for the ejected-energy differential and total cross sections for the electron-impact ionization of he-

lium [23]. Good agreement has also been demonstrated between experiment and total ionization cross-section calculations for Li^+ [24], carbon, and neon [25]. In Sec. II, we give a summary of the time-dependent close-coupling theory; in Sec. III, we present our total integral and ejected-energy differential cross sections for the electron-impact ionization of lithium; and in Sec. IV, we summarize and reach conclusions.

II. THEORY

A. Time-dependent close-coupling method

The time-dependent close-coupling theory has been discussed in some detail in studies of the electron-impact ionization of hydrogen [21,22]. Here we outline only the main points of the theory.

The $1s^2$ ground state of Li^+ is calculated in the Hartree-Fock approximation. A set of bound $\bar{n}l$ and continuum $\bar{k}l$ radial orbitals is then obtained by diagonalization of the one-dimensional Hamiltonian given by

$$h(r) = -\frac{1}{2}\frac{\partial^2}{\partial r^2} + \frac{l(l+1)}{2r^2} - \frac{Z}{r} + V_D(r) + V_X(r), \quad (1)$$

where $V_D(r)$ and $V_X(r)$ are the direct Hartree and local exchange potentials, respectively, Z is the nuclear charge of the target, and atomic units are used throughout. These potentials are calculated using the $1s$ orbital, and a parameter in the exchange term is adjusted so that the single-particle energies for each angular momentum are in good agreement with the configuration-average experimental spectrum. A pseudopotential is used to generate a $\bar{2}s$ orbital that eliminates the inner node of the wave function and problems associated with core superelastic scattering [4]. The $\bar{2}s$ pseudo-orbital is very similar to the $2s$ orbital found from a Hartree-Fock calculation for the $1s^2 2s$ ground state of lithium.

At a time $t=0$ before the collision, two-electron radial wave functions $P_{l_1 l_2}^{LS}(r_1,r_2,t)$ are given by antisymmetrized or symmetrized spatial products of the $\bar{2}s$ orbital and an incoming radial wave packet, where we define L as the total orbital angular momentum, S as the total spin angular momentum ($S=0$ or 1), and where (l_1,l_2) are the angular momenta for the target and initial scattered electrons (or the ejected and final scattered electrons). Their time propagation is governed by the time-dependent Schrödinger equation, which takes the form

$$i\frac{\partial P_{l_1 l_2}^{LS}(r_1,r_2,t)}{\partial t} = T_{l_1 l_2}(r_1,r_2)P_{l_1,l_2}^{LS}(r_1,r_2,t)$$

$$+ \sum_{l_1',l_2'} U_{l_1 l_2, l_1' l_2'}^{L}(r_1,r_2)P_{l_1' l_2'}^{LS}(r_1,r_2,t), \quad (2)$$

where $T_{l_1 l_2}(r_1,r_2)$ contains kinetic energy, centrifugal bar-

rier, nuclear, direct Hartree and local exchange operators, and $U_{l_1 l_2, l_1' l_2'}^{L}(r_1,r_2)$ couples the various $(l_1 l_2)$ scattering channels.

Finite differencing methods are used to represent the close-coupled partial differential equations on a 300×300 point lattice with a uniform mesh spacing $\Delta r_1 = \Delta r_2 = 0.30$ a.u. Each radial wave function is propagated in time using an explicit second-order differencing scheme. At a time $t=T$ following the collision, the two-electron radial wave functions may be projected onto products of the $\bar{n}l$ orbitals to extract collision probabilities and thus inelastic cross sections. The radial wave functions are propagated until all collision probabilities have converged.

For ejected-energy differential cross sections, the two-electron radial wave functions are projected onto the $\bar{k}l$ continuum radial orbitals to yield momentum space probabilities. Plots of the absolute value squared of the wave function in radial and momentum space are shown in Figs. 1(a) and 1(b), for the ^1S partial wave with $l_1=l_2=0$ at time $t=80$ a.u. after the collision. It is clear that the elastically scattered part of the wave function travels much faster than any other part and reflects back into the box at 90 a.u. By this stage, the wave packet along $r_1=r_2$, which represents ionization, is well away from the core so that this reflection does not affect the ionization probabilities. In the (k_1,k_2) plane, the momentum space probabilities are peaked along a ridge of total energy $E=k_1^2/2+k_2^2/2=E_0-I_P$, where E_0 is the incident electron energy and I_P is the ionization potential.

Dividing the (k_1,k_2) plane into angular segments, defined by the hyperspherical angle $\tan(\theta)=k_2/k_1$, allows us to define the partial differential cross section as

$$\frac{d\sigma(LS)}{d\theta} = \frac{\pi}{k^2}\frac{(2L+1)(2S+1)}{4}$$

$$\times \sum_{l_1,l_2}\int_0^\infty dk_1 \int_0^\infty dk_2 \,\delta\left(\theta - \tan^{-1}\frac{k_2}{k_1}\right)$$

$$\times \left|\int_0^\infty dr_1 \int_0^\infty dr_2 P_{\bar{k}_1 l_1}(r_1)P_{\bar{k}_2 l_2}(r_2)\right.$$

$$\left.\times P_{l_1 l_2}^{LS}(r_1,r_2,t)\right|^2. \quad (3)$$

The partial differential cross section in ejected energy may be obtained from the simple transformation

$$\frac{d\sigma(LS)}{d\epsilon} = \frac{1}{k_1 k_2}\frac{d\sigma(LS)}{d\theta}, \quad (4)$$

and the partial integral cross section is then

$$\sigma(LS) = \int_0^E \frac{d\sigma(LS)}{d\epsilon}d\epsilon. \quad (5)$$

Finally the total integral cross section is given by

$$\sigma = \sum_{LS} \sigma(LS). \qquad (6)$$

We may also define a partial spin asymmetry parameter, $\mathcal{A}(L)$, as

$$\mathcal{A}(L) = \frac{\sum_{L'=0}^{L} \left[\sigma(L'S=0) - \frac{1}{3}\sigma(L'S=1) \right]}{\sum_{L'=0}^{L} \sum_{S=0}^{1} \sigma(L'S)}, \qquad (7)$$

where the total spin asymmetry parameter is given by

$$\mathcal{A} = \lim_{L \to \infty} \mathcal{A}(L). \qquad (8)$$

B. Distorted-wave theory

The distorted-wave theory for electron-impact ionization of atoms is based on a triple partial-wave expansion of the first-order perturbation theory scattering amplitude [26]. The total cross section is given by

$$\sigma = \frac{16}{k_i^3} \int_0^E \frac{d\epsilon}{k_e k_f} \sum_{l_i, l_e, l_f} (2l_i+1)(2l_e+1)$$
$$\times (2l_f+1)\mathcal{P}(l_i, l_e, l_f, k_i, k_e, k_f), \qquad (9)$$

where the linear momenta (k_i, k_e, k_f) and the angular momentum quantum numbers (l_i, l_e, l_f) correspond to the incoming, ejected, and outgoing electron, respectively, and $\mathcal{P}(l_i, l_e, l_f, k_i, k_e, k_f)$ is the first-order scattering probability.

The $2s$ orbital is generated from a Hartree-Fock calculation for the $1s^2 2s$ ground state of lithium. The incoming and outgoing scattered electron is calculated in a V^N potential, while the ejected electron is calculated in a V^{N-1} potential, where $N=3$ is the number of electrons in the target. The distorted-wave calculations presented in this paper include both direct and exchange terms in the scattering amplitude. This expression gives the configuration-average cross section and a simple modification of the angular algebra allows spin-resolves partial-wave cross sections to be extracted.

III. RESULTS

Partial-wave ionization cross sections for electron scattering from lithium, calculated using both the time-dependent close-coupling method and time-independent distorted-wave method, are presented in Table I for four incident electron energies. Both calculations use an experimental ionization potential of 5.39 eV [27]. The distorted-wave results contain both direct and exchange terms in the scattering potential. We find that, for most energies and partial waves, the distorted-wave results are higher than the close-coupling results, resulting in a higher distorted-wave total cross section compared to the close-coupling total cross section for each incident electron energy.

The time-dependent close-coupling equations for the two-electron radial wave functions are solved on a numerical lattice as described in the preceding section. The total time propagation of the wave function is determined by the con-
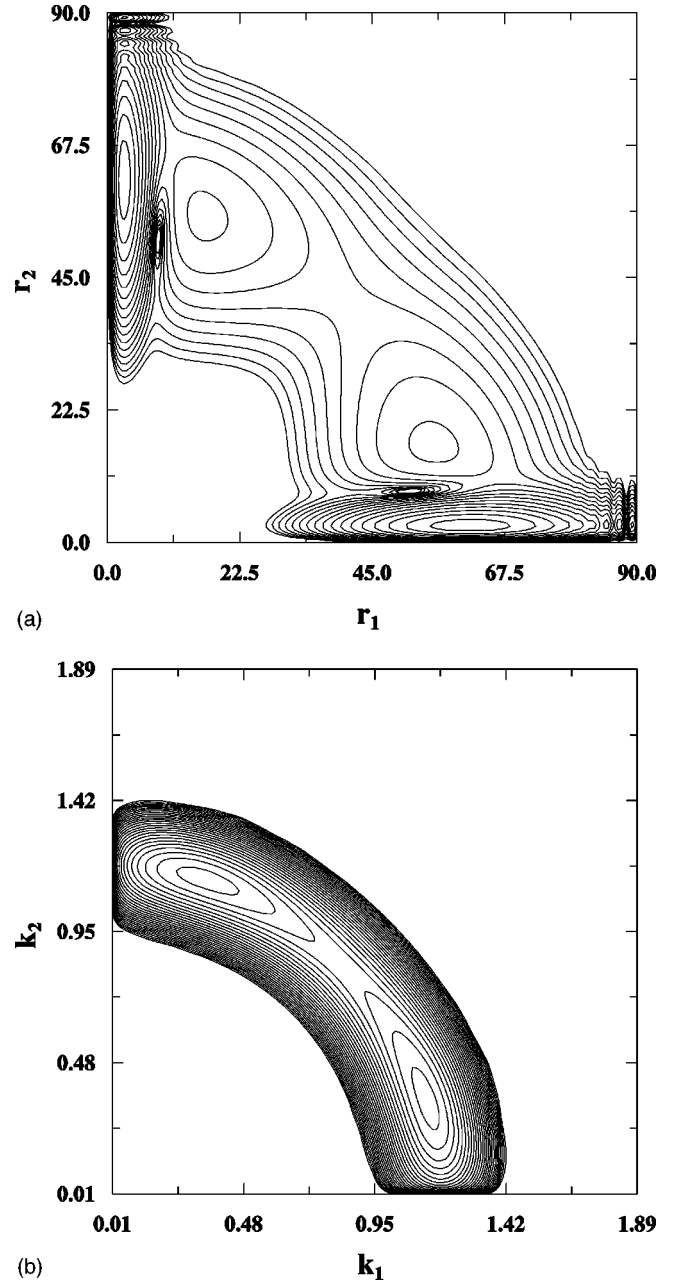

FIG. 1. (a) Contour plot of $|P_{l_1 l_2}^{LS}(r_1, r_2, T)|^2$, where $L=S=l_1=l_2=0$ and $T=80$ a.u. for an incident energy of 25.4 eV. (b) Contour plot of $|\int_0^\infty dr_1 \int_0^\infty dr_2 P_{k_1 l_1}(r_1) P_{k_2 l_2}(r_2) P_{l_1 l_2}^{LS}(r_1, r_2, T)|^2$, where $L=S=l_1=l_2=0$ and $T=80$ a.u. for an incident energy of 25.4 eV. (Distances r_1, r_2 and momenta k_1, k_2 are in atomic units.)

vergence of the collision probabilities; in general, shorter times are needed for larger incident energies. The number of $(l_1 l_2)$ coupled channels ranges from 4 for $L=0$ to 22 for $L=6$. For the highest $L=10$ angular momentum calculations carried out at an incident electron energy of 15 eV, it was necessary to include 27 $(l_1 l_2)$ coupled channels for convergence in angular momenta.

Total ionization cross sections for electron scattering from lithium at low incident electron energies are presented in Fig. 2. The solid diamonds with error bars are the experimental measurements of Zapesochnyi and Aleksakhin [10] (which

TABLE I. Partial ionization cross sections (Mb) for lithium at four incident electron energies. (TDCC denotes time-dependent close-coupling method, DW denotes distorted-wave method, L denotes total orbital angular momentum, 1.0 Mb$=1.0\times10^{-18}$ cm^2.)

| L | 10 eV | | 15 eV | | 20 eV | | 25.4 eV | |
	TDCC	DW	TDCC	DW	TDCC	DW	TDCC	DW
0	4.7	24.3	5.4	18.7	5.1	12.7	4.6	8.5
1	36.4	88.0	30.9	60.6	23.2	42.8	17.9	31.3
2	48.7	79.1	46.2	63.8	37.6	41.4	30.1	40.8
3	43.2	117.4	42.4	62.5	36.4	45.1	31.1	36.7
4	52.1	86.5	49.6	76.9	40.8	55.7	34.1	41.5
5	46.1	48.6	49.5	63.2	42.2	53.8	35.4	42.4
6	30.1	24.0	41.4	44.0	39.4	44.6	35.0	39.0
0–6	261.3	467.9	265.4	389.7	224.7	296.1	188.2	240.2
7–50		20.5		69.4		112.6		121.4
0–50		488.4		459.1		408.7		361.6

do not extend beyond 30 eV), and the dashed line is the convergent close-coupling calculations of Bray [2]. The other experimental measurements of McFarland and Kinney [11] and Jalin *et al.* [12] do not begin until higher energies, well away from the peak of the cross section. The solid squares are time-dependent close-coupling results, where the results have been ''topped-up'' at the higher angular momentum ($L\geq7$) by distorted-wave results. Also shown are time-independent distorted-wave results where direct and exchange terms are included in the scattering potential (solid line). These distorted-wave calculations are in good agreement with earlier distorted-wave calculations of Younger [9]. We see that the time-dependent close-coupling results are in excellent agreement with the convergent close-coupling cal-

culations in this energy range, but are substantially lower than the experimental measurements of Zapesochyni and Aleksakhin [10]. We also note that both nonperturbative calculations are in good agreement with the binary-encounter-dipole model calculations of Kim [29].

In Fig. 3, we present time-dependent close-coupling calculations of ejected-energy differential cross sections for electron scattering from lithium at four incident electron energies. The close-coupling calculations are ''topped-up'' at higher angular momentum ($L\geq6$) with time-independent distorted-wave calculations. The ejected electron energy has been normalized to aid presentation [i.e., (normalized ejected energy)=(ejected energy)/(total energy)]. As expected, the ejected-energy differential cross sections are all symmetric
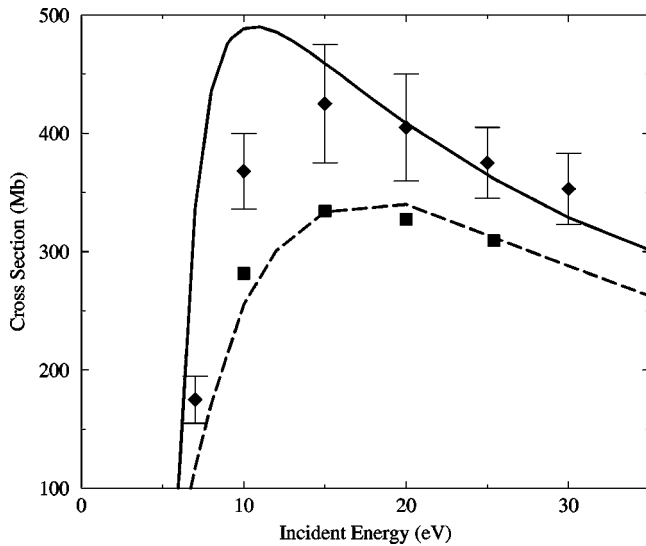

FIG. 2. Total electron-impact ionization cross section for electron scattering from lithium. Solid squares: time-dependent close-coupling method, solid line: distorted-wave method, dashed line: convergent close-coupling method [2], solid diamonds with error bars: experiment [10]. (1.0 Mb$=1.0\times10^{-18}$ cm^2.)
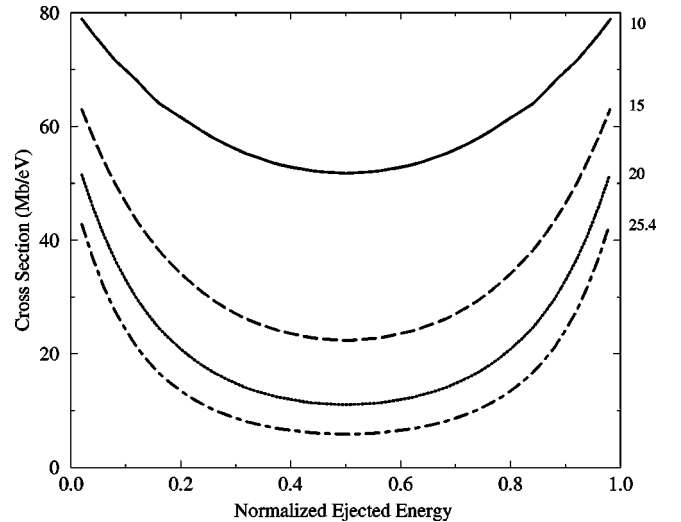

FIG. 3. Ejected-energy differential cross sections for electron scattering from lithium at four incident electron energies. Time-dependent close-coupling method, solid line: 10 eV, long-dashed line: 15 eV, short-dashed line: 20 eV, dot-dashed line: 25.4 eV. (Normalized ejected energy = ejected energy/total energy, 1.0 Mb$=1.0\times10^{-18}$ cm^2.)
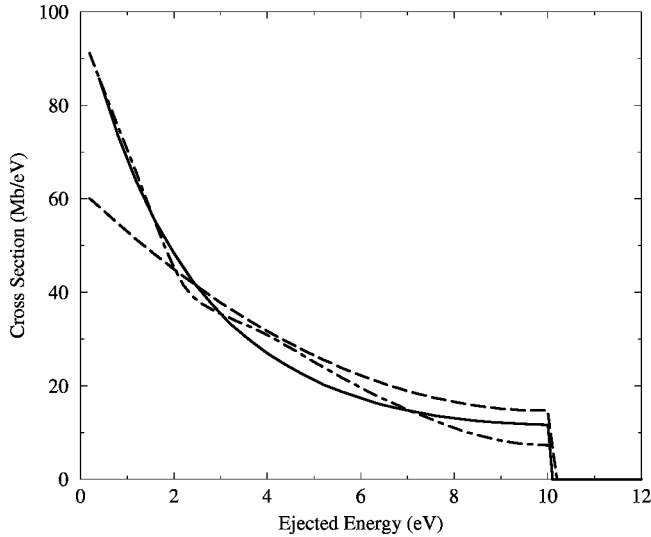
FIG. 4. Ejected-energy differential cross section for electron scattering from lithium at an incident energy of 25.4 eV. Solid line: Time-dependent close-coupling method, dot-dashed line: converged close-coupling method using 107 states [13], dashed curve: extrapolated converged close-coupling method [13]. (1.0 Mb$=1.0$ $\times 10^{-18}$ cm^2.)

about $E/2$, where E is the total energy. We note also that the ejected-energy differential cross section is significantly flatter at lower incident electron energies, which is in agreement with recent studies of near-threshold ejected-energy differential cross sections of electron scattering from hydrogen [20].

To compare with the ejected-energy differential cross-section calculations of Bray *et al.* [13], we plot in Fig. 4 our ejected-energy differential cross section at 25.4 eV, where we have multiplied the cross section by 2 and plotted from 0 to $E/2$. This is done to facilitate comparison with the convergent close-coupling method, in which the ejected-energy differential cross section is extracted in such a way that results are obtained from 0 to $E/2$ only. Our results are multiplied by a factor of 2 so that we compare equal areas under the differential cross-section curves (i.e., so that total cross sections are the same).

The solid line shows the time-dependent close-coupling results at 25.4 eV as described previously. The dot-dashed line is the converged close-coupling results obtained using 107 states as described by Bray *et al.* [13]. The dashed line is an extrapolation of the converged close-coupling results to suggest a fully converged calculation [13]. We see that the time-dependent close-coupling results fall between these two curves and that the agreement overall is only moderately good.

Spin-resolved partial-wave cross sections at an incident electron energy of 15 eV are presented in Table II calculated using the time-dependent close-coupling and time-independent distorted-wave approaches, along with the corresponding partial spin asymmetry parameter. We note that, by $L=6$, the ratio of the cross section from the triplet to singlet partial waves is still a long way from the statistical ratio of 3, for both the time-dependent close-coupling and distorted-wave calculations. We have therefore extended our

TABLE II. Spin-resolved partial ionization cross sections (Mb) and partial spin asymmetry parameter [$\mathcal{A}(L)$] for lithium at 15 eV incident electron energy. (TDCC denotes time-dependent close-coupling method, DW denotes distorted-wave method, L denotes total orbital angular momentum, S denotes total spin angular momentum, 1.0 Mb$=1.0\times10^{-18}$ cm^2.)

^{2S+1}L	TDCC (Mb)	$\mathcal{A}$ (L)	DW (Mb)	$\mathcal{A}$ (L)
^{1}0	3.6		14.8	
^{3}0	1.7	0.57	3.9	0.72
^{1}1	12.7		34.8	
^{3}1	18.1	0.27	25.8	0.50
^{1}2	34.0		42.9	
^{3}2	12.2	0.48	20.9	0.53
^{1}3	27.0		29.2	
^{3}3	15.4	0.49	33.3	0.46
^{1}4	32.8		30.8	
^{3}4	16.8	0.51	46.1	0.39
^{1}5	25.2		25.6	
^{3}5	24.2	0.47	37.7	0.35
^{1}6	16.4		18.2	
^{3}6	25.0	0.43	25.8	0.34
^{1}7	10.3		11.6	
^{3}7	19.8	0.40	16.6	0.33
^{1}8	6.5		7.0	
^{3}8	14.0	0.38	9.8	0.33
^{1}9	4.1		3.8	
^{3}9	9.5	0.37	6.5	0.32
^{1}10	2.6		1.9	
^{3}10	6.3	0.36	4.2	0.32
0–10	338.2		451.2	
11–50			8.2	
0-50			459.1	

time-dependent close-coupling calculations to $L=10$, for this energy only, to follow the ratio of the triplet to singlet cross sections. By $L=10$, the triplet to singlet ratio is much closer to the statistical value of 3. For the distorted-wave calculation, it was found that increasing the number of orbital angular momenta l_e did make a small difference in the individual spin-resolved partial wave cross sections at high L, but that this made virtually no difference to the partial spin asymmetry parameter $\mathcal{A}(L)$. We see that the individual distorted-wave partial wave cross sections are still some way off the time-dependent close-coupling results, even at $L=10$. Previous studies [28] have shown that the convergence of distorted-wave calculations is slow even for singly and doubly charged ions. In the current case, neutral Li, it may be necessary to calculate individual partial wave cross sections for up to $L=20$ to obtain good agreement between the time-dependent and time-independent methods.

On the other hand, $\mathcal{A}(L)$ oscillates for low values of the total orbital angular momentum, but does converge as high

TABLE III. Total spin asymmetry parameter ($\mathcal{A}$) for lithium at 15 eV incident electron energy. (TDCC denotes time-dependent close-coupling method, CCC denotes converged close-coupling method [2], Expt. denotes experiment [30].)

	$\mathcal{A}$
TDCC	0.36
CCC	0.35
Expt.	0.39

orbital angular momentum values are reached. It is clear that calculation of the spin-resolved partial wave cross sections up to high values of the orbital angular momentum $L = 10$ is necessary to achieve convergence in the spin asymmetry parameter. To compare with other calculations and experiment, Table III shows the final spin asymmetry parameter calculated at 15 eV using the time-dependent close-coupling method for $L = 0 - 10$. We see that there is excellent agreement with the convergent close-coupling calculation of Bray [2], and that both theoretical calculations are slightly lower than the experiment of Baum *et al.* [30].

IV. SUMMARY

This paper reports total integral and ejected-energy differential cross sections for the electron-impact ionization of lithium, using the well-known time-dependent close-coupling method [21,22]. Total integral cross sections are found to be in excellent agreement with the convergent close-coupling calculations of Bray [2] and with binary-encounter-dipole calculations of Kim [29], and are substan-

tially lower than the experimental measurements of Zapesochnyi and Aleksakhin [10] made over 25 years ago. New experiments measuring the total cross section for the electron-impact ionization of lithium could perhaps bring theory and experiment into better agreement.

Ejected-energy differential cross sections, calculated at an incident electron energy of 25.4 eV, are found to be in only moderately good agreement with convergent close-coupling calculations, in the energy range 0 to $E/2$, where E is the total energy. We also present ejected-energy differential cross sections at other incident electron energies (10, 15, and 20 eV) for which there are no other nonperturbative theoretical or experimental comparisons available. It is hoped that this paper will stimulate experimental work in this area in order that nonperturbative theory may be tested more fully.

Finally, the spin asymmetry parameter at an incident electron energy of 15 eV is found to be in excellent agreement with convergent close-coupling calculations, and in very good agreement with the experimental measurements of Baum *et al.* [30]. It is found that time-dependent calculations of spin-resolved partial-wave cross sections must be carried out for a large number of orbital angular momenta to obtain convergence in the partial spin asymmetry parameter.

[1] L. E. Zakharov, http://w3.pppl.gov/zakharov/ LiWalls001025.html, *Mini-conference on Lithium Walls and Low Recycling Regimes in Tokamaks*, Intl. Cong. on Plasma Physics, Quebec City, Canada (2000).

[2] I. Bray, J. Phys. B **28**, L247 (1995).

[3] K. Bartschat and I. Bray, J. Phys. B **30**, L109 (1997).

[4] M. S. Pindzola, F. Robicheaux, N. R. Badnell, and T. W. Gorczyca, Phys. Rev. A **56**, 1994 (1997).

[5] P. J. Marchalant, K. Bartschat, and I. Bray, J. Phys. B **30**, L435 (1997).

[6] O. Woitke, N. Djuric, G. H. Dunn, M. E. Bannister, A. C. H. Smith, B. Wallbank, N. R. Badnell, and M. S. Pindzola, Phys. Rev. A **58**, 4512 (1998).

[7] D. M. Mitnik, M. S. Pindzola, D. C. Griffin, and N. R. Badnell, J. Phys. B **32**, L479 (1999).

[8] R. A. Falk and G. H. Dunn, Phys. Rev. A **27**, 754 (1983).

[9] S. M. Younger, J. Quant. Spectrosc. Radiat. Transf. **26**, 329 (1981).

[10] I. P. Zapesochnyi and I. S. Aleksakhin, Zh. Éksp. Teor. Fiz. **55**, 76 (1968) [Sov. Phys. JETP **28**, 41 (1969)].

[11] R. H. McFarland and J. D. Kinney, Phys. Rev. **137**, A1058 (1965).

[12] R. Jalin, R. Hagemann, and R. Botter, J. Chem. Phys. **59**, 952 (1973).

[13] I. Bray, J. Beck, and C. Plottke, J. Phys. B **32**, 4309 (1999).

[14] M. Streun, G. Baum, W. Blask, J. Rasch, I. Bray, D. V. Fursa, S. Jones, D. H. Madison, H. R. J. Walters, and C. T. Whelan, J. Phys. B **31**, 4401 (1998).

[15] M. Streun, G. Baum, W. Blask, and J. Barakdar, Phys. Rev. A **59**, R4109 (1999).

[16] X. Zhang, C. T. Whelan, and H. R. J. Walters, J. Phys. B **25**, L457 (1992).

[17] F. Boudali, B. Najjari, and B. Joulakian, J. Phys. B **33**, 2383 (2000).

[18] T. N. Rescigno, M. Baertschy, W. A. Isaacs, and C. W. Mc-Curdy, Science **286**, 2474 (1999).

[19] I. Bray, J. Phys. B **33**, 581 (2000).

[20] M. Baertschy, T. N. Rescigno, C. W. McCurdy, J. Colgan, and M. S. Pindzola, Phys. Rev. A **63**, 050701(R) (2001).

[21] M. S. Pindzola and D. R. Schultz, Phys. Rev. A **53**, 1525 (1996).

[22] M. S. Pindzola and F. Robicheaux, Phys. Rev. A **54**, 2142 (1996).

[23] M. S. Pindzola and F. Robicheaux, Phys. Rev. A **61**, 052707 (2000).

[24] M. S. Pindzola, D. M. Mitnik, J. Colgan, and D. C. Griffin, Phys. Rev. A **61**, 052712 (2000).

[25] M. S. Pindzola, J. Colgan, F. Robicheaux, and D. C. Griffin, Phys. Rev. A **62**, 042705 (2000).

[26] S. M. Younger, in *Electron Impact Ionization*, edited by T. D. Mark and G. H. Dunn (Springer-Verlag, Berlin, 1985), p. 1.

[27] *Atomic Energy Levels I*, edited by C. E. Moore, Natl. Bur. Stand. U.S. NSRDS No. 35 (U.S. GPO, Washington, DC, 1971).

[28] N. R. Badnell, M. S. Pindzola, I. Bray, and D. C. Griffin, J. Phys. B **31**, 911 (1998).

[29] Y. K. Kim (private communication).

[30] G. Baum, M. Moede, W. Raith, and W. Schroder, J. Phys. B **18**, 531 (1985).